

---

# Non-linear command of wind turbine based on doubly-fed induction generator

**Zakaria Sabiri<sup>1</sup>, Nadia Machkour<sup>1</sup>, Mohammed Bezza<sup>1</sup>, Elm'kaddem Kheddioui<sup>1</sup>, David Ouoba<sup>2</sup>**

*1. Laboratory of Physics of Atmosphere, Materials and Modeling  
Faculty of Sciences and Technology of Mohammadia,  
Hassan II University of Casablanca Mohammadia, Morocco  
sabiri.zakaria@gmail.com*

*2. Laboratory of Physics and Condensed Matter and Renewable Energy  
Faculty of Sciences and Technology of Mohammadia,  
Hassan II University of Casablanca Mohammadia, Morocco*

---

*ABSTRACT. the topic's work is the modeling and control of a variable speed wind turbine based on the asynchronous doubly-Fed Induction generator DFIG. The goal is to control separately the active and reactive power of the generator with the backstepping method, using the Lyapunov functions to ensure system stability. A simulation of the control law using Matlab/Simulink was made to verify its validity.*

*RÉSUMÉ. Ce travail porte sur la modélisation et le contrôle d'une éolienne à vitesse variable basée sur la génératrice asynchrone à double alimentation GADA. L'objectif est de commander séparément la puissance active et réactive de la génératrice avec la méthode backstepping, en utilisant les fonctions de Lyapunov pour assurer la stabilité du système. Une simulation de la loi de commande utilisant le logiciel Matlab/Simulink a été faite pour vérifier sa validité.*

*KEYWORDS: wind turbine, doubly-Fed Induction generator (DFIG), MPPT, backstepping.*

*MOTS-CLÉS : éolienne, génératrice asynchrone à double alimentation (GADA), backstepping, MPPT.*

---

DOI:10.3166/EJEE.18.385-397 © Lavoisier 2016

## 1. Introduction

For a few years now, renewable energy systems have been used to generate electrical energy that is transferred by an electric network on relatively long distances to users. They are suitable to locations where access to the public network is difficult. Thus, there are two types of connection of these hybrid systems (Quang, 2014): the first is connected to the grid, and the second, called autonomous, is used in places which cannot be connected thereto (the grid).

Our project deals with the study of a hybrid system based on wind turbine, photovoltaic (PV) panels and batteries in order to inject the energy produced in an island or rural electric network. The proposed configuration is showed in Figure 1.

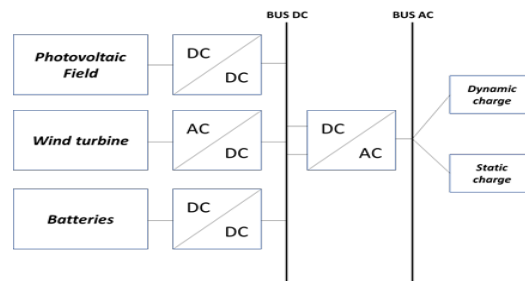


Figure 1. Global structure

In this architecture, we study separately each element of the assembly, PV, wind turbine or storage system in order to connect each one to a normalized DC Bus. In this work, we will focus only on the control of the wind turbine. In our case, we use a horizontal axis wind turbine which is based on a Doubly fed Induction generator DFIG. To control it, there are two methods: MPPT and PQ methods.

The objective of the MPPT control strategy is to extract the maximum wind power, this extraction is indicated by a maximum power factor. Moreover, this control will be able to perform a correction of the power factor by producing or consuming reactive energy (Frédéric, 2003; Hilal, 2014; Belghazi, 2015).

Concerning the PQ control, it is used for different power ranges, which is based on vector control with stator flux orientation to decouple the active and reactive power of the DFIG. The objective of the PQ command (Active and Reactive Power Setpoint) is to produce active and reactive powers that equalize the references provided by the power grid manager in order to control the wind turbine.

The research work of (Hilal, 2014) are focused on the comparison between the MPPT and PQ commands. The results obtained showed a good tracking of reference with the PQ command compared to MPPT command. But, the fixed active power references require that the wind turbine draws its stored energy to be able to enslave

the power to its reference. This will happen when the power provided by the turbine is below the desired setpoint.

To control the wind turbine, many methods were developed. Some of them are linear using PI corrector (Hong *et al.*, 2010; Koutroulis *et al.*, 2006) and others are based on a non-linear control using some usual techniques such as: fuzzy logic (Huynh *et al.*, 2011) and Sliding mode (Beltran *et al.*, 2008).

The objective of this work is to mix the two commands MPPT and PQ. This is to bless the advantages of the PQ command in the setpoint tracking, and the realistic reference coming from the MPPT command according to the variation of the wind. This paper proposes a robust control scheme for a wind turbine equipped with a DFIG. The proposed robust design uses the Backstepping control method to regulate the active and reactive power on the rotor-side, and to bring the energy produced back to the DC bus in the stator-side. Figure 2 describes the wind turbine connection diagram with the standard 800V DC bus (Sabiri *et al.*, 2014).

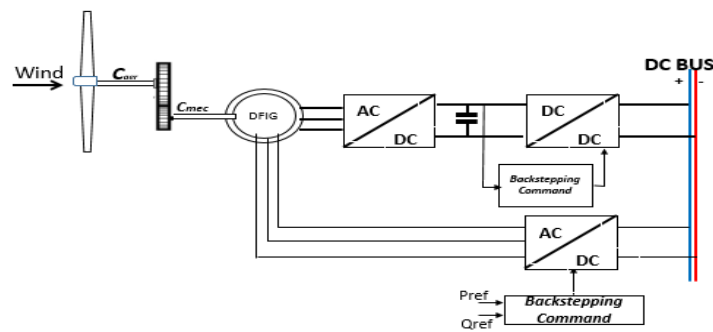


Figure 2. Wind turbine connection with the DC bus

## 2. System modeling

The studied system consists of a wind turbine based on a DFIG with nominal power 15KW, a stator side converter controlled by the Backstepping method, which is used to control the active and reactive power of the machine. To connect the turbine to selected DC bus, two static converters were placed stator side, the first one is a type double rectifier bridge 3, and the second one is a double BOOST chopper controlled by the Backstepping method in order to stabilize and maintain the voltage rectified in the desired bus voltage, which is 800V. The modeling of the mechanical system is recommended to study our system. Then, the processing of the various blocks of the conversion chain will be mentioned.

### 2.1. Modeling of a wind turbine

The power extracted by the wind turbine is calculated by (1), where  $C_p$  is the power coefficient whose theoretical limit is 0.59 (Neris *et al.*, 1999),  $\lambda$  is the specific speed,  $\rho$  is the air density,  $S$  is the swept area by the pale and  $V$  is wind speed.

$$P_{turbine} = 0.5 \rho C_p(\lambda, \beta) S V^3 \quad (1)$$

The expression of the power coefficient is given by Equation (2), where  $\beta$  is the angle pitch of the turbine (Frédéric, 2003).

$$C_p(\lambda, \beta) = [0.5 - 0.00167 \times (\beta - 2)] \times \sin \left[ \frac{\pi(\lambda + 0.1)}{18.5 - 0.3 \times (\beta - 2)} \right] - 0.00184(\lambda - 3)(\beta - 2) \quad (2)$$

The mechanical torque of the wind turbine is obtained from the extracted power from wind. It is defined by (3), where  $\Omega_t$  is the rotational speed of the turbine.

$$C_{mec} = \frac{Peol}{\Omega_t} \quad (3)$$

The machine is adapted to the turbine *via* a speed gain multiplier  $G$ . The resulting equation is presented by

$$C_{mec} = \frac{1}{G} C_t \quad (4)$$

The generator shaft is modeled by the following equation:

$$J \frac{d\Omega}{dt} = C_{mec} - C_{em} - f\Omega \quad (5)$$

With:  $J$ : Total inertia of the rotating part;  $f$ : Coefficient of viscous friction;  $C_{em}$ : Electromagnetic torque of the generator.

### 2.2. MPPT Command of wind turbine

The Control of the speed of DFIG requires a reference speed, which is managed through the technique of MPPT (Neris *et al.*, 1999). This reference depends on the wind speed  $V$ , the multiplier gain  $G$ , the maximum specific speed  $\lambda_{opt}$  and  $R$  blades radius. The speed reference is given by the equation:

$$\Omega_{ref} = \frac{\lambda_{opt} \cdot V \cdot G}{R} \quad (6)$$

The reference is compared with the speed of the generator for estimating the electromagnetic torque through a PI controller. Figure 3 shows the speed control loop.

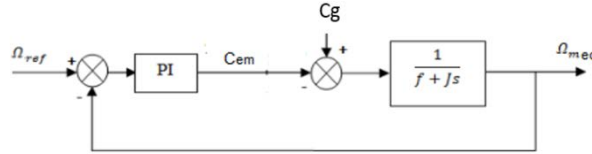


Figure 3. Regulation of mechanical speed

The parameters of the PI controller are defined by the Equation (7):

$$\begin{cases} K_p = 2 \cdot \xi \cdot \omega_{nd} \cdot J - f \\ K_i = \omega_{nd}^2 \cdot J \end{cases} \quad (7)$$

$\xi = 0.7$  And  $\omega_{nd} = \frac{4.75}{t_{sd}}$ . With  $t_{sd}$  is the response time of the system.

### 2.3. Backstepping controller for DFIG

#### 2.3.1. In the rotor side

The *Backstepping* method is based on the reporting of errors in functions of system parameters and instructions and lowering them (errors) to a zero value by applying a control law respecting the *Lyapunov* stability conditions (Koutroulis *et al.*, 2006; Kaldellis *et al.*, 2007; Bouallegue *et al.*, 2016).

The equations defining the system are (El Majdoub *et al.*, 2015; Kanchanaharuthai *et al.*, 2016):

$$\begin{cases} P_s = -V_s \cdot \frac{M}{L_s} \cdot I_{qr} \\ Q_s = -V_s \cdot \frac{M}{L_s} \cdot I_{dr} + V_s \cdot \frac{\phi_s}{L_s} \\ \dot{I}_{qr} = \frac{1}{\sigma} \cdot V_{qr} - S_1 \\ \dot{I}_{dr} = \frac{1}{\sigma} \cdot V_{dr} - S_2 \end{cases} \quad (8)$$

With:

$$\begin{cases} S_1 = \frac{1}{\sigma} \left( R_r \cdot I_{qr} - g \cdot w_s \cdot \gamma \cdot I_{dr} - g \frac{M \cdot V_s}{L_s} \right) \\ S_2 = \frac{1}{\sigma} \left( -R_r \cdot I_{dr} + g \cdot w_s \cdot \gamma \cdot I_{qr} \right) \\ \sigma = L_r - \frac{M^2}{L_s} \\ \gamma = L_s - \frac{M^2}{L_s} \end{cases} \quad (9)$$

With M is the mutual inductance.

Step 1: definition of the first error:

$$\begin{cases} \varepsilon_1 = P_{ref} - P_s \\ \varepsilon_2 = Q_{ref} - Q_s \end{cases} \quad (10)$$

With Pref is the reference for active power and Qref is the reference for reactive power. The derivative of the error with respect to time leads to

$$\begin{cases} \dot{\varepsilon}_1 = \dot{P}_{ref} - \dot{P}_s \\ \dot{\varepsilon}_2 = \dot{Q}_{ref} - \dot{Q}_s \end{cases} \quad (11)$$

The first Lyapunov function is defined by:

$$V_1 = \frac{1}{2} (\varepsilon_1^2 + \varepsilon_2^2) \quad (12)$$

Deriving this function and respecting the stability condition of the Lyapunov function, the first stabilizing functions  $\alpha_1$  system and  $\alpha_2$  are calculated by:

$$\begin{cases} \alpha_1 = \frac{L_s \cdot \sigma}{V_s \cdot M \cdot R_r} \left( k_1 \cdot \varepsilon_1 + \dot{P}_{ref} + \frac{V_s M}{L_s \sigma} \left( V_{qr} - g \cdot w_s \cdot \gamma \cdot I_{dr} - g \frac{M \cdot V_s}{L_s} \right) \right) \\ \alpha_2 = \frac{L_s \cdot \sigma}{V_s \cdot M \cdot R_r} \left( k_2 \cdot \varepsilon_2 + \dot{Q}_{ref} + \frac{V_s M}{L_s \sigma} \left( V_{dr} - g \cdot w_s \cdot \gamma \cdot I_{qr} \right) \right) \end{cases} \quad (13)$$

With  $k_1$  and  $k_2$  are the Backstepping coefficients and are strictly positive.

Step 2: involves the definition of  $\varepsilon_3$  and  $\varepsilon_4$  errors as follows:

$$\begin{cases} \varepsilon_3 = \alpha_1 - I_{qr} \\ \varepsilon_4 = \alpha_2 - I_{dr} \end{cases} \quad (14)$$

The second Lyapunov function is described by:

$$V_2 = V_1 + \frac{1}{2} (\varepsilon_3^2 + \varepsilon_4^2) \quad (15)$$

Deriving the Lyapunov function and respecting its stability condition, we get the control law as follows:

$$\begin{cases} V_{qr} = \sigma \left( k_3 \cdot \varepsilon_3 + \dot{\alpha}_1 - S_1 \right) \\ V_{dr} = \sigma \left( k_4 \cdot \varepsilon_4 + \dot{\alpha}_2 - S_2 \right) \end{cases} \quad (16)$$

Thus, the figure shows the control loop for active and reactive power (Hilal *et al.*, 2011; Payam *et al.*, 2014).

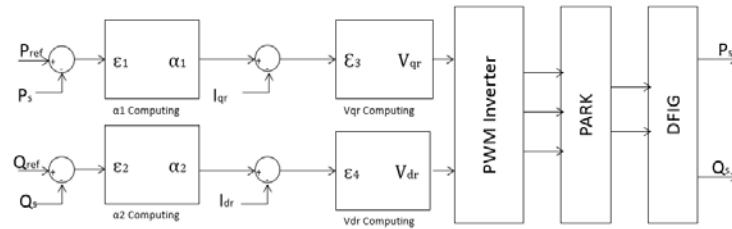


Figure 4. Global control system of DFIG

2.3.2. In the sotor side

The command to the stator allows the transfer of the power generated at the DC bus via two static converters. The first one is a bridge rectifier (Figure 5). It is used to reduce the voltage produced by the DFIG continuous signal.

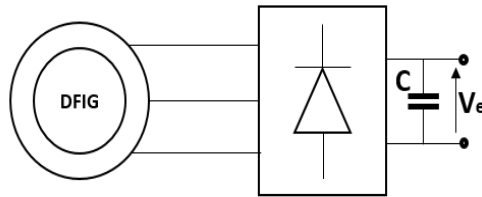


Figure 5. Schema of DC/DC converter

The second is a double boost chopper (Figure 6), controlled by the Backstepping method (Sabiri *et al.*, 2015; 2014). Its control law is given by Equation (17):

$$\dot{u} = \frac{1-u}{\alpha} \left[ \left( \frac{1-u}{L} - \frac{K_{c1}^2 \cdot L}{1-u} \right) \varepsilon_{c1} + (-K_{c1} - K_{c2}) \varepsilon_{c2} - \frac{2}{RC} V_{DC} - \frac{2(1-u)}{c} i_1 + \frac{L}{1-u} \ddot{I}_{co} \right] \quad (17)$$

With:

$$\varepsilon_1 = i_1 - I_{co} \tag{18}$$

$$I_{co} = \frac{V^2_{co}}{R \cdot V_e} \tag{19}$$

$$\varepsilon_2 = V_{DC} - \alpha \tag{20}$$

$$\alpha = \frac{K_{c1} \cdot L \cdot \varepsilon_1 + V_e - L \cdot \dot{I}_{co}}{1 - u} \tag{21}$$

$K_{c1}$  and  $k_{c2}$  are the Backstepping coefficients controller for double boost chopper and are strictly positive.

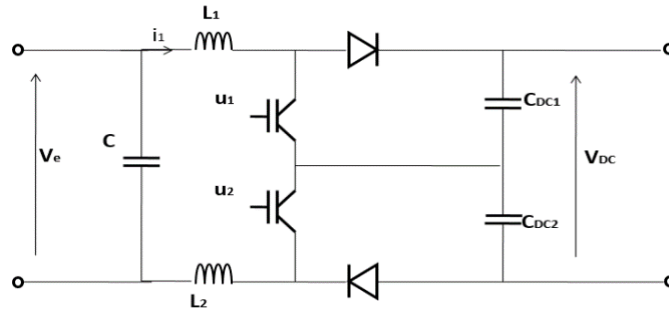


Figure 6. Double Boost converter

### 3. Simulation and Discussion

The DFIG is placed in the nearest operating conditions of a wind system. The studied wind turbine is an average power one, so the angle  $\beta$  is assumed to be fixed. The goal of MPPT command is to extract the maximum power from wind energy. The parameters of the DFIG are describe on the Table 1.

Table 1. Generator Parameter

Variable	Value	Variable	Value
Vs	400V	Lm	0.1212 H
$\omega_s$	$2 \times \pi \times 50$	Ps	15KW
Rs	0.2147 $\Omega$	$\Omega_s$	1500 tr/min
Rr	0.2205 $\Omega$	K1	9900
p	2	K2	9800
Ls	0.0290 H	K3	8500
Lr	0.0290 H	K4	10000

Thus, the command applied to the inverter magnetizing generator imposes the desired active power output, while the reactive power must be zero. On Stator side, two static converters are positioned to connect wind turbine to the DC bus. Figure 7 depicts the block diagram of the wind turbine.

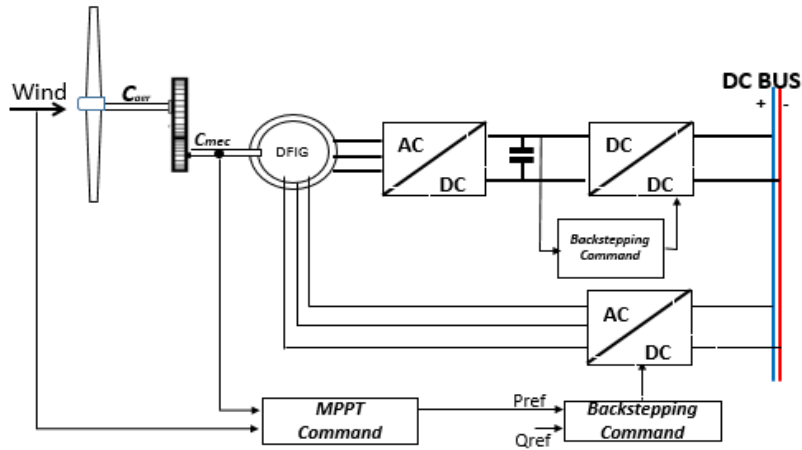


Figure 7. Structure with MPPT

The wind speed is supposed variable, Figure 6, to test the validity of our model. The following figures show the simulation results obtained:

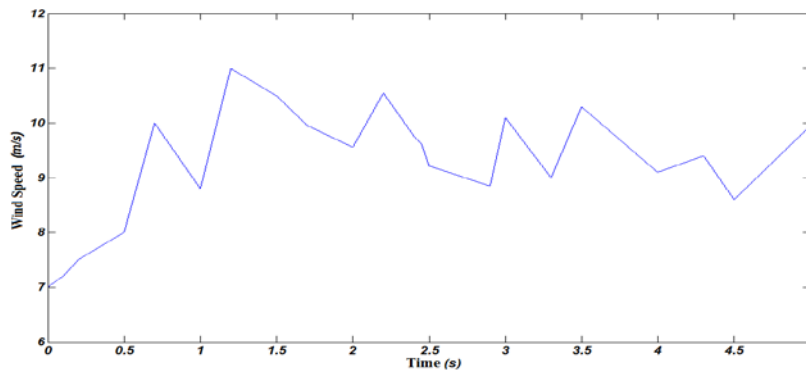


Figure 8. Wind Speed

Figures 9 and 10 show the efficiency of the wind turbine control strategy, the Betz coefficient  $C_p$  is maintained at its maximum value 0.52 while  $\lambda$  to maximum 9.6 at  $\beta=0$ . The measurement of the active power from the DFIG is shown

in Figure 11. and we note the correct tracking of the reference power point. The average error is calculated at  $P_{moy}=48.4527W$ . while the reactive power is kept constant at its reference null. The reactive average error is calculated  $Q_{moy}=20VAR$ . The overall performance of the command is calculated to  $\eta=98.65\%$  which is largest comparing to other commands (Huynh *et al.*, 2012). The wind turbine is provided connected with the 800V DC bus via the converters connected to the stator as shown in Figure 13.

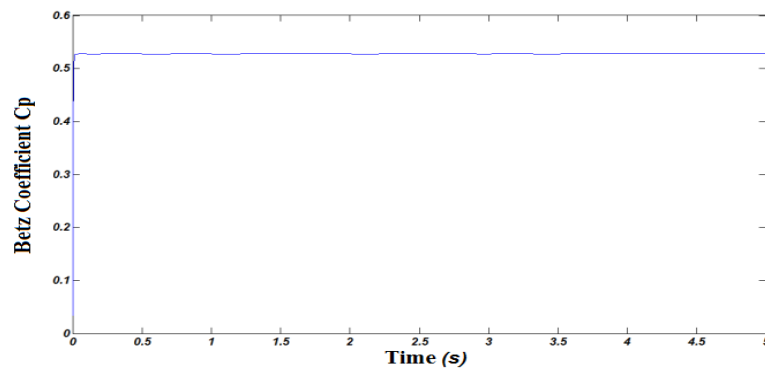


Figure 9. Variation of Betz coefficient Cp

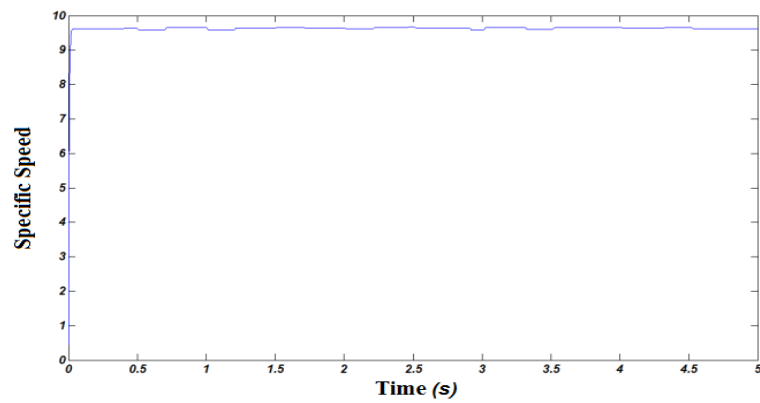


Figure 10. Specific Speed Lambda

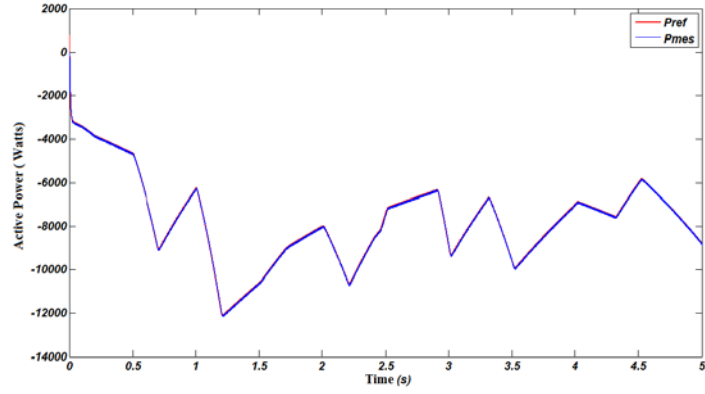


Figure 11. Active power

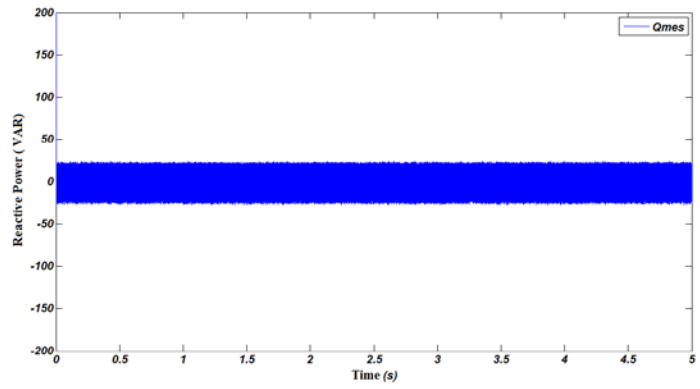


Figure 12. Reactive power

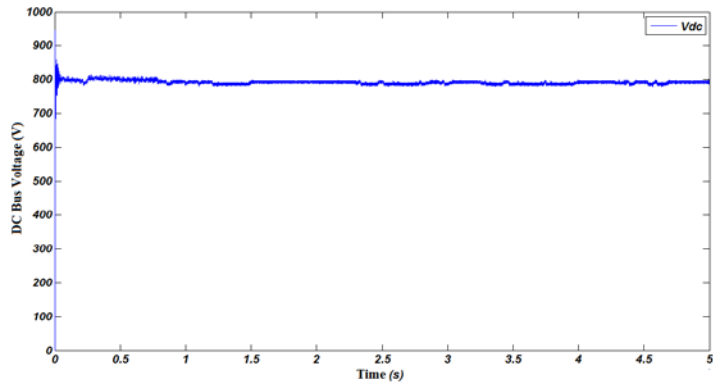


Figure 13. Voltage  $V_{DC}$

#### 4. Conclusion

Using the Matlab/Simulink environment, we have tested the validity of the command system of a wind turbine based on DFIG. The Backstepping controller is used to command the different power converters composing the system. The simulation results have shown a good convergence and response stability of the different blocs of the system, regardless of the climatic circumstances. This is explained by the high performance of production that is superior to 99%, in comparison with other methods used in the literature, such as fuzzy logic (Huynh *et al.*, 2011), P&O (Neris *et al.*, 1999).

As a perspective, we plan to connect the wind generator with a photovoltaic field in order to have a hybrid system in order to study the efficiency and other performances of the Backstepping method as a MPPT technic.

#### References

- Neris A.S., Vovos N.A., Giannakopoulos G.B. (1999). A Variable Speed Wind Energy Conversion Scheme for Connection to Weak AC Systems. *IEEE Transactions on Energy Conversion*, vol. 14, n° 1, March, p. 122-127.
- Beltran B., Ahmed-Ali T., and Benbouzid M.E.H. (2008). "Sliding mode power Control of variable speed wind energy conversion systems," *IEEE Trans. Energy Convers.*, vol. 23, n° 22, p. 551-558, June .
- Frédéric P. (2003). Etude et commande de génératrices asynchrones pour l'utilisation de l'énergie éolienne-machine asynchrone a cage autonome-machine asynchrone à double alimentation reliée au réseau. Thèse de doctorat. Université de Nantes.
- Bouallegue S., Khoud K. (2016). Integral Backstepping Control Prototyping for a Quad Tilt Wing Unmanned Aerial Vehicle, *International Review of Aerospace Engineering (IREASE)*, vol. 9, n° 5, p. 152-161.
- El Majdoub, K., Ouadi (2015). Backstepping Control for Semi-Active Suspension of Half-Vehicle with Dahl Magnetorheological Damper Model. *International Journal on Engineering Applications (IREA)*, vol. 3, n° 4, p. 96-107.
- Huynh Q., Nollet F., Essounbouli N., Hamzaoui A. (2011). Power management of a variable speed wind turbine for stand-alone system using fuzzy logic. In *Fuzzy Systems (FUZZ), 2011 IEEE International Conference on*, p. 1404-1410. IEEE.
- Huynh Q., Nollet, F., Essounbouli, N., Hamzaoui, A. (2012). Fuzzy control of variable speed wind turbine using permanent magnet synchronous machine for stand-alone system. In *Sustainability in Energy and Buildings. Proceedings of the 3rd International Conference in Sustainability in Energy and Buildings (SEB 11)*, vol. 12, p. 31. Springer Verlag.
- Kaldellis J., Kavadias K., Koronakis P. (2007). *Comparing wind and photovoltaic stand-alone power systems used for the electrification of remote consumers. Renewable and Sustainable Energy Reviews*, vol. 11, n° 1, p. 57-77.

- Kanchanaharuthai A., Mujjalinvimut E. (2016). An Adaptive Backstepping Coordinated Excitation and STATCOM Control for Power Systems. *International Review of Electrical Engineering (IREE)*, vol. 11 n° 4, p. 391-398.
- Koutroulis E. and Kalaitzakis K. (2006). Design of a maximum power tracking system for wind-energy-conversion applications. *Industrial Electronics, IEEE Transactions on*, vol. 53, n° 2, p. 486-494.
- Hilal M., Benchagra M., Errami Y., Maaroufi M., Ouassaid M. (2011). Maximum power tracking of wind turbine based on doubly fed induction generator. *International Review of Modelling and Simulations*, vol. 4 n° 5, p. 2255-2263, October.
- Quang M.H. (2014). Optimisation de la production d'électricité pour site isolé," these University Reims-champagne ardeins.
- Payam A., Hassani F., Fathipour M. (2014). Design of Hybrid Closed Loop Control Systems for a MEMS Accelerometer Using Nonlinear Control Principles. *International Review of Aerospace Engineering (IREASE)*, vol. 7, n° 5, p. 164-170.
- Sabiri Z., Machkour N., Kheddioui Elm., Boujoudi B., Camara M.B., Dakyo B. (2015). DC/DC converters for the conditioning of Photovoltaic energy- Modeling and command strategy. *American Journal of Engineering Research AJER*, vol. 4, n° 2, feb.
- Sabiri Z., Machkour N., Elm. Kheddioui, Camara M.B., Dakyo B. (2014). DC/DC converters for Photovoltaic Applications- Modeling and Simulations. *Proceeding conference IRSEC Ouarzazate-17-19 October*.

